Dalton Transactions

Accepted Manuscript

This is an *Accepted Manuscript*, which has been through the Royal Society of Chemistry peer review process and has been accepted for publication.

Accepted Manuscripts are published online shortly after acceptance, before technical editing, formatting and proof reading. Using this free service, authors can make their results available to the community, in citable form, before we publish the edited article. We will replace this *Accepted Manuscript* with the edited and formatted *Advance Article* as soon as it is available.

You can find more information about *Accepted Manuscripts* in the Information for Authors.

Please note that technical editing may introduce minor changes to the text and/or graphics, which may alter content. The journal's standard Terms & Conditions and the Ethical guidelines still apply. In no event shall the Royal Society of Chemistry be held responsible for any errors or omissions in this *Accepted Manuscript* or any consequences arising from the use of any information it contains.

ROYAL SOCIETY OF CHEMISTRY

www.rsc.org/dalton

Crystal Lattice Effect on the Quenching of the Intracluster Magnetic Interaction in $[V_{12}B_{18}O_{60}H_6]^{10-}$Polyoxometalate.

*Patricio Hermosilla-Ibáñez,[a,b] Walter Cañon-Mancisidor, [a,b] Juan Costamagna,[a] Andrés Vega,[b,c] Verónica Paredes-García,[b,c] Maria Teresa Garland,[d] Eric Le Fur,[e,f] Olivier Cador,[g] Evgenia Spodine,[*b,h] and Diego Venegas-Yazigi,[*a,b].*

[a]*Facultad de Química y Biología, Universidad de Santiago de Chile, Chile. USACH*

[b] *CEDENNA, Chile.*

[c]*Universidad Andres Bello, Departamento de Ciencias Químicas, Facultad de Ciencias Exactas, Chile.*

[d]*Facultad de Ciencias Físicas y Matemáticas, Universidad de Chile, Chile.*

[e]*ENSCR, CNRS, UMR 6226, Rennes, France.*

[f]*Université Européenne de Bretagne, France.*

[g]*Institut des Sciences Chimiques de Rennes, UMR 6226 CNRS, Université de Rennes1, Rennes, France.*

[h]*Facultad de Ciencias Químicas y Farmacéuticas, Universidad de Chile, Chile.*

Dalton Transactions Accepted Manuscript

ABSTRACT

In the present work, the synthesis and structural characterization of four new polyoxovanadoborates (BVO) frameworks, based on the $[V_{12}B_{18}O_{60}H_6]^{10-}$ polyanion are reported: $(NH_4)_8(1,3\text{-diap}H_2)[V_{12}B_{18}O_{60}H_6]\cdot 5.24H_2O$ (**1**), $K_8(NH_4)_2[V_{12}B_{18}O_{60}H_6]\cdot 18.00H_2O$ (**2**), $K_{10}[V_{12}B_{18}O_{60}H_6]\cdot 9.50H_2O$ (**3**) and $K_8Cs_2[V_{12}B_{18}O_{60}H_6]\cdot 10.40H_2O$ (**4**). A global antiferromagnetic behaviour is observed for these $10V^{IV}/2V^{V}$ mixed valence clusters. The magnetic data of **1**, **2** and **3**, which present different countercation environment, show that **1** is more coupled than **2** and **3**. DFT calculations show that the positive charges strongly influence the polarization mechanism of the spin density of the vanadyl groups and the extent of the magnetic orbitals, therefore corroborating the experimental observation of the quenching effect of the magnetic coupling between vanadium centres of **2** and **3**.

KEYWORDS: Polyoxometalate, Mixed Valence, BVO, Magnetic Properties, DFT, Quenching of Antiferromagnetism, Spin Polarization Mechanism.

Dalton Transactions Accepted Manuscript

INTRODUCTION

During the last decades, polyoxometalates (POMs) have attracted a great scientific interest due to their structural variety and chemical properties. They present applications in catalysis, optics, magnetism, medicine and electrochemistry among others [1-20]. A recently investigated family of POMs is the polyoxovanadoborate (BVO) [21], which presents different vanadium/boron stoichiometries and different mixed valence V^{IV}/V^{V} ratios. Several frameworks have been reported in the literature with different V/B stoichiometry, and in which ethylenediamine and 1,3-diaminopropane, with different degree of protonation, are present in the crystalline lattice [22-31]. Some of the reported BVO clusters stabilize their negative charge not only with amines with different degrees of protonation, but also with cations, and hydronium ions. These charge compensating species are also acting as connectors, increasing the dimensionality of the system from 0D to 1D, 2D or 3D. However, the existence of frameworks based on the connectivity of BVO clusters exclusively by alkaline ions is scarce, and to the best of our knowledge only two pure inorganic frameworks of this type have been reported up to date, $Rb_4[(VO)_6\{B_{10}O_{16}(OH)_6\}_2]\cdot 0.5H_2O$ [32], and $Na_{10}[(H_2O)V_{12}B_{18}O_{60}H_6]\cdot 18H_2O$ [33].

The magnetic properties of some mixed valence POMs have been studied, classifying these compounds in systems in which the unpaired electrons are localized or delocalized all over the metal centres of the structure [34]. On the other hand, Gatteschi et al. reported that the magnitude of the exchange interaction and therefore the overall magnetic properties of the V_{18} system, depend on the number of V^{IV} atoms present in the polyanion. This is evidenced by the significant decrease of the magnetic moment per centre, when the number of paramagnetic centres decreases in the polyanion [4,35]. For the $[V_{12}B_{18}O_{60}H_6]^{n-}$ systems the magnetic properties have been only

Dalton Transactions Accepted Manuscript

briefly described, indicating that antiferromagnetic interactions exist in the aforementioned cluster, without a thorough analysis of the effect of the alkaline ions in the crystalline lattice on the corresponding magnetic behaviour [36].

In order to study the effect of the nature of the cations present in the lattice based on the $[V_{12}B_{18}O_{60}H_6]^{10-}$ polyanion on the electronic and magnetic properties, the synthesis, structural characterization, UV-visible spectra and DFT calculations of four new polyoxovanadoborates (BVO) frameworks with the same mixed valence ratio are reported: $(NH_4)_8$(1,3-diapH_2)$[V_{12}B_{18}O_{60}H_6]\cdot 5.24H_2O$ (**1**), $K_8(NH_4)_2[V_{12}B_{18}O_{60}H_6]\cdot 18.00H_2O$ (**2**), $K_{10}[V_{12}B_{18}O_{60}H_6]\cdot 9.50H_2O$ (**3**) and $K_8Cs_2[V_{12}B_{18}O_{60}H_6]\cdot 10.40H_2O$ (**4**).

Dalton Transactions Accepted Manuscript

EXPERIMENTAL SECTION

SYNTHESES OF COMPOUNDS

All chemicals were reagent grade and used without further purification. Compound **1** was prepared in a 23 mL teflon lined Parr reactor, by heating at 180ºC for 5 days, while compounds **2** to **4** were also obtained in a 23 mL teflon lined Parr reactor, but heating at 170ºC for 3 days. After cooling to room temperature, dark red crystals of **1**, **2**, **3** and **4**, were collected by filtration. The crystals were washed with water and dried at room temperature.

$(NH_4)_8$(1,3-diapH_2)[$V_{12}B_{18}O_{60}H_6$]·5.24H_2O (**1**). A mixture of V_2O_5 (0.1818 g, 1.00 mmol), H_3BO_3 (1.0000 g, 16.0 mmol), $(NH_4)_2HPO_4$ (0.1981 g, 1.50 mmol), H_2O (2.0 mL, 111 mmol) and 1,3-diaminopropane (0.4 ml, 6.00 mmol) was used to obtain **1.** The initial pH value of the reacting mixture was 11.61 and the final pH value was 10.20. Yield: (0.0500 g, 14% based on V). ICP analysis shows that the V content (28.97%) is consistent with the stoichiometry.

$K_8(NH_4)_2$[$V_{12}B_{18}O_{60}H_6$]·18.00H_2O (**2**). A mixture of NH_4VO_3 (0.2164 g, 1.85 mmol), $K_2B_4O_7·4H_2O$ (1.5092 g, 4.94 mmol), H_2O (2.0 mL, 111 mmol) and ethylenediamine (0.08 mL, 1.24 mmol) was used to prepare **4.** Initial pH was 10.80 and the final value was 10.63. Yield: (0.1530 g, 40% based on V). ICP analysis shows that the molar ratio of V:K of 11.96:8.07, which is consistent with the stoichiometry.

Dalton Transactions Accepted Manuscript

$K_{10}[V_{12}B_{18}O_{60}H_6]\cdot 9.50H_2O$ (**3**). A mixture of KVO_3 (0.2554 g, 1.85 mmol), $K_2B_4O_7\cdot 4H_2O$ (1.5092 g, 4.94 mmol), H_2O (2.0 mL, 111 mmol) and ethylenediamine (0.08 mL, 1.24 mmol) was used to obtain **5.** Initial pH value was 10.90 and the final one 10.80. Yield: (0.1047 g, 28% based on V). ICP analysis shows that the molar ratio of V:K of 11.98:10.13, which is consistent with the stoichiometry.

$K_8Cs_2[V_{12}B_{18}O_{60}H_6]\cdot 10.40H_2O$ (**4**). A mixture of $CsVO_3$ (0.4288 g, 1.85 mmol), $K_2B_4O_7\cdot 4H_2O$ (1.5092 g, 4.94 mmol), H_2O (2.0 mL, 111 mmol) and ethylenediamine (0.08 mL, 1.24 mmol) was used to obtain **6**. Initial pH was 9.00 and the final one 10.90. Yield: (0.0507 g, 13% based on V). ICP analysis shows that the molar ratio of V:K:Cs of 11.95:8.02:1.97, which is consistent with the stoichiometry.

CRYSTAL STRUCTURE DETERMINATION.

For each compound a single crystal was taken directly from the synthesis vessel. Examination under microscope suggested acceptable quality; these were mounted on the tip of a glass fibre. Preliminary examination with X-rays confirmed the quality suggested by microscopy, proceeding to full data collection. The intensities for **1**, **2**, **3** and **4** were recorded at room temperature on a Bruker Smart Apex diffractometer, using separations of 0.3° between frames and 10s by frame. Data integration were made using SAINTPLUS [37]. The structures were solved by direct methods using XS in SHELXTL [38] and completed (non-H atoms) by Fourier difference synthesis. Refinement until convergence was obtained using XL SHELXTL [39] and SHELXL97 [40]. The H-atom positions were calculated after each cycle of refinement using a riding model, with C—H = 0.97 Å and $U_{iso}(H) = 1.2\ U_{eq}$(parent) and N—H = 0.89 or 0.91 Å and $U_{iso}(H) = 1.5$

Dalton Transactions Accepted Manuscript

U_{eq}(parent). Efforts to locate the borovanadate H atoms in the final Fourier difference map were unsuccessful; those reported for the formula are based on charge-balance analysis. For compound **1** the 5.24 oxygen atoms, corresponding to solvating intermolecular water molecules were modelled using partial occupations (refined and then held constant) over 12 different positions. No hydrogen atoms from the ammonium ions or water were located in the final difference Fourier map. For compound **2** the occupancy of potassium atoms are 0.91 (K1), 0.84 (K2), 0.62 (K3) and 0.63 (K4). For compound **3** the occupancies were refined and then held constant at 0.80 (K1), 0.50/0.20 (K2A/K2B), 0.80 (K5) and 0.30/0.40 (K6A/K6B), while for compound **4** the occupancy of potassium and caesium atoms are 0.75 (K2), 0.75 (K3), 0.50 (K6), 0.42/0.08 (Cs1A/Cs1B) and 0.50 (Cs2). Efforts for lowering the rather high residuals on the refinement for each compound included the evaluation of different models of solvation, and the use of squeeze for the modelling of the remaining density was unsuccessful. Some parameters remained high; this should be considered as arising from the complexity of the model used for the solvation and counterbalancing. Moreover, it is not related to the main characteristics of the structures, whose determination should still be considered as correct. For the crystallographic description, distances up to 3.1 Å were considered to define hydrogen bonds in the crystalline lattice [41]. Structure drawings were carried out with DIAMOND-3.2i, supplied by Crystal Impact [42]. Crystallographic data for structures of **1** to **4** reported in this paper, have been deposited with the Cambridge Crystallographic Data Centre as supplementary publication number CCDC-932256, 963463, 963464, 963465. Copies of the data can be obtained free of charge on application to CCDC, 12 Union Road Cambridge CB21EZ, UK (Fax: int. code +44 (123) 336-033; E-mail: deposit@ccdc.cam.ac.uk

Dalton Transactions Accepted Manuscript

In order to describe the geometries around the alkaline ions found in the different frameworks, the methodology of the continuous shape measures algorithm [43], the minimal distortion paths [44], and the generalized interconversion coordinates [45] were used, as established in the SHAPE Code [46].

ICP ANALYSES

The chemical analysis of vanadium, potassium, caesium were carried out using inductively coupled plasma (ICP) methods on an ICP–OES Perkin–Elmer, Optima 3300 DV analyzer.

THERMOGRAVIMETRIC ANALYSES

Thermogravimetric analyses (TGA) of (**1**), (**2**), (**3**) and (**4**) were performed from room temperature to 700ºC, under a nitrogen atmosphere with a heating rate of 1ºC min^{-1}, using a Netzsch thermogravimetric analyzer, model 209-F1.

SPECTROSCOPICAL MEASUREMENTS

IR spectra of the compounds were determined on a Perkin Elmer FT-IR spectrophotometer, model BX II, from 4000 to 400 cm^{-1} using KBr pellets. The UV-vis spectra for **1** to **4** were obtained at room temperature in the range of 200-850 nm using a Lambda 1050 Wideband UV-vis-NIR Spectrophotometer, equipped with a diffuse reflectance attachment (Biconical DRA-CA-50M).The absorbance values were obtained by the use of the Kubelka-Munk function [47].

Dalton Transactions Accepted Manuscript

MAGNETIC MEASUREMENTS

The magnetic susceptibility measurements for **1**, **2** and **3** were obtained on ground polycrystalline samples, in the temperature range of 2-300 K with a Quantum Design MPMS-XL5 SQUID magnetometer with an applied *dc* field of 5 kOe. The susceptibility data were corrected for the diamagnetic contributions of the sample using Pascal´s constants [48].

COMPUTATIONAL DETAILS

DFT calculations of the exchange interaction in a dinuclear oxovanadium model system, considering the effect of alkaline atoms.

The crystalline structure of $[V_2O_2(\mu_2\text{-}OH)_2(1,4,7\text{-triazacyclononane})_2]^{2+}$(CINKUF, CCDC code) [49] was used as a model structure to evaluate the effect of surrounding alkaline ions on the magnetic interaction between the bridged V^{IV} atoms. For this purpose two M^+ ions (M = Na, K) were placed symmetrically above the two oxygen atoms of the vanadyl groups at distances of 3.5, 4, 5, 6, 7 and 8 Å. For these model systems the magnetic exchange interaction was calculated for each case. Long distances were used in order to check the influence of the electric field generated by the presence of the cation in the network, thus avoiding bonding interactions.

Spin-unrestricted calculations under the Density Functional Theory approach were done, using the hybrid B3LYP functional [50] and a triple-ζ all electron basis set for all atoms [51]. A guess function was generated using Jaguar 5.5 code [52], using a triple-ζ basis set for all atoms. Total energy calculations were performed with the Gaussian09 program [53], using the quadratic convergence method with a convergence criterion of 10^{-7} a.u.. Mulliken spin densities were obtained from the single point calculations.

Dalton Transactions Accepted Manuscript

The Heisenberg-Dirac-van Vleck spin Hamiltonian was used to describe the exchange coupling in the polynuclear complex:

$$\hat{H} = -\sum_{i>j} J_{ij} \hat{S}_i \hat{S}_j$$

where S_i and S_j are the spin operators of the paramagnetic centres i, j of the compound. The J_{ij} parameters are the magnetic coupling constants between the centres i, j with unpaired electrons of the molecule. Finally, the *J* value was obtained using the non-projected method proposed by Ruiz et al.[54].

$$E_{HS} - E_{BS} = -(2S_1S_2 + S_2)J$$

where S_1 and S_2 are the total spins of the two interacting paramagnetic centres with $S_1 \geq S_2$.

RESULTS AND DISCUSSION

SYNTHESES OF THE $V_{12}B_{18}O_{60}H_6$ SYSTEMS

The preparation of the framework **1** was done at 180ºC for 5 days. At lower temperatures (170 ºC) and fewer days of reaction (3 days) framework **1** was not obtained, as was the case of **2** to **4**.

For all the obtained compounds a diamine was added to the reaction media. However, only **1** presents protonated amines in the crystalline framework, while for the rest of the crystalline lattices, **2** to **4**, the added diamine was not part of the final framework, and the obtained lattices are totally inorganic. This fact could be related, as stated above, to the temperature used in the

Dalton Transactions Accepted Manuscript

syntheses, since the crystalline frameworks **2** to **4** are only formed when prepared at 170 °C. On the other hand, since the initial vanadium source is a vanadium (V) precursor, the used diamine acts as a reducing agent in all the studied compounds. This observation was corroborated by qualitative analyses using ionic liquid chromatography for **1** to **4**, where nitrate ions were detected in the mother liquors.

THERMOGRAVIMETRIC ANALYSES.

Figure S1 shows the TG analyses of compounds **1** to **4**. The thermogram of compound **1** shows a weight loss of 13.3% between 25 and 221ºC, being the calculated value for 4.24 water molecules plus 8 ammonia molecules and one 1,3-diap 13.7% of weight loss. It is possible to observe that the thermograms of compounds **2** to **4** show a continuous weight loss between room temperature and 700 °C, which clearly corresponds to the loss of water molecules and the decomposition of each compound. No relevant information can be obtained from these curves. It is interesting to point out that **1**, being the compound containing protonated amines and therefore the highest number of hydrogen bond interactions, is the only one that has a marked weight loss.

FT-IR SPECTROSCOPIC ANALYSIS.

Compounds **1** to **4** present similar spectra, since their crystalline structure is based on the same anionic unit $[V_{12}B_{18}O_{60}H_6]^{10-}$ with the same degree of oxidation. The characteristic bands for these types of structures are: ν_{B-O} (BO_3), ν_{B-O} (BO_4), ν_{V-O}, $\nu_{V=O}$. It is interesting to stress that the V=O band located at c.a. 950 cm^{-1} presents an asymmetric shape for all the compounds, and this feature could be due to the different interactions of the vanadyl groups in the lattice (Figures S2 and S3). It has been published before by Müller et al.[35] that the energy of the V=O band depends

Dalton Transactions Accepted Manuscript

on the mixed valence ratio. In this work it is possible to observe that the crystalline lattice effect plays also a role in the position of the stretching band.

Framework **1** that contains protonated amines has a spectrum with ν_{C-H} (CH_2), ν_{N-H}, vibration modes corresponding to the aliphatic amines; ν_{O-H} due to the water molecules present in the lattice of all compounds can also be detected. The summary of these absorption bands is given in Table S1.

REFLECTANCE UV-VISIBLE SPECTRA

Due to the insolubility of all studied compounds, the solid diffuse reflectance UV-visible spectra were recorded (Figure 1). All the studied compounds crystallize as dark red crystals and gave similar UV-visible spectra, as previously reported by Hermosilla-Ibañez et al.[55]. The absorption band centred at 555 nm observed for the four studied compounds was assigned to an intervalence charge transfer transition (IVCT) between the V^{IV}/V^{V} centres of the polyoxovanadoborate unit. The absorption bands which appear in the high energy UV region were assigned to the charge transfer O→V band at 240 nm for **1**, 252 nm for **2**, 231 for **3** and 239 for **4**, and to the charge transfer O→B band at 322 nm for **1**, 324 nm for **2**, 321 nm for **3** and 319 nm for **4**, as reported by Zhou et al.[56]. Therefore, the electronic absorptions observed in the solid state seem to be dependent only on the polyoxovanadoborate moiety, and the characteristics of the lattice have little influence on the optical properties.

GENERAL COMMENTS ON THE CRYSTAL STRUCTURES

Dalton Transactions Accepted Manuscript

Crystal data and structure refinement for complexes **1-4** are listed in Table 1. The crystalline lattice of compounds **1** to **4** is based on the $[V_{12}B_{18}O_{60}H_6]^{10-}$ polyanion. This polyanion is formed by the condensation of two hexanuclear units of oxovanadate $[V_6O_9]^{7+}$ with a $[B_{18}O_{36}(OH)_6]^{24-}$ borate ring. This ring is located in the centre of the cluster, which contains an occluded water molecule (Figure S4). All the vanadium atoms have a distorted square base pyramidal geometry, while the boron atoms adopt both, trigonal (B_{trig}) and tetrahedral (B_{tet}) geometries, with V=O, V-O, B_{trig}-O and B_{tet}-O bond distances and O=V-O, O-B_{trig}-O and O-B_{tet}-O angles, which are in the range of reported values in the literature [33,55].

Structural description of $(NH_4)_8(1,3\text{-}diapH_2)[V_{12}B_{18}O_{60}H_6]\cdot 5.24H_2O$ (1).

The framework of **1** shows that the polyanions $[V_{12}B_{18}O_{60}H_6]^{10-}$ are counterbalanced by ammonium, and 1,3-propilendiammonium cations (1,3-diapH_2), which presents hydrogen bond interactions in the crystalline lattice. Besides being a countercation, the 1,3-diapH_2 links polyanionic clusters through hydrogen bonds. Figure S5 shows the different types of hydrogen bonds (unidirectional, bifurcated and trifurcated) generated by the ammonium groups of the 1,3-diapH_2 in the crystalline lattice.

Each 1,3-diapH_2 is oriented along the *c* axis (Figure 2), and connected to four $[V_{12}B_{18}O_{60}H_6]^{10-}$ clusters by different hydrogen bonds (Figure S6). It is interesting to stress that the use of the branched 1,2-diapH_2, as reported by Liu et al. [57] does not permit the preferential orientation of the organic cations in the lattice, as is observed in **1**. The values for the most representative hydrogen bonds for **1** are given in Table S2. All these interactions permit to define a supramolecular structure.

Dalton Transactions Accepted Manuscript

The ammonium ions in the crystal structure present four different crystallographic sites, N2, N3, N4 and N5 (Figure S7). The first ammonium ion (N2) and the last one (N5) connect three BVO clusters, while the second (N3) and the third (N4) connect two POM units. All the N···O donor/acceptor interactions are in the range of 2.710 Å to 3.096 Å.

Structural description of $K_8(NH_4)_2[V_{12}B_{18}O_{60}H_6]\cdot 18.00H_2O$ (2).

The crystalline lattice of **2** contains five crystallographically different potassium ions, four of them hexa-coordinated (K1, K2, K4, K5) and one hepta-coordinated (K3). The ions K2 and K4 are coordinated to two polyanionic clusters, while K1, K5 and K3 are bonded to three BVO moieties, even though the latter is hepta-coordinated. All the potassium ions interact with oxygen atoms from the vanadyl groups, terminal oxygen atoms of B_{trig} and oxygen atoms from a borate bridging group. K1 completes its coordination sphere with two water molecules, while K2, K3 and K4 with three, whereas K5 does it with oxygen atoms from the polyanionic units. All distances related to this analysis are given as supplementary material (Table S3).

Figure S8-a shows the location of the alkaline ions along the *b* axis, while Figure S8-b shows the alternating ABABA position of the polyanionic ligands along this same axis. The clusters present AAAAA or BBBBB order along the *a* axis. In this way, the interstitial space is filled by the potassium ions, which are coordinated to the BVO clusters, generating a 3D crystalline order.

Structural description of $K_{10}[V_{12}B_{18}O_{60}H_6]\cdot 9.50H_2O$ (3).

Dalton Transactions Accepted Manuscript

The crystalline lattice of **3** is formed by six different crystallographic sites for the potassium ions, with K2 and K6 presenting disorder. As already mentioned, K2A/K2B and K6A/K6B were considered having occupancies of 0.5/0.2 and 0.3/0.4 respectively.

The hepta-coordinated sphere of K1 is formed by three oxygen atoms from one anionic cluster, two oxygen atoms from a second anionic cluster and two water molecules (The corresponding distances are given as supplementary material). For the description of the coordination sphere of K2 the occupancy of K2A was considered as predominant, and an octahedral environment is described. K2A binds three polyanionic species and two water molecules. The corresponding distances are given as supplementary material. K3 is also hexa-coordinated, connecting two different POMs and two water molecules. K4 presents a hexa-coordinated environment, having two bonds to one POM and three bonds to a second cluster, completing the hexa-coordination with a water molecule. K5 is connected to three POM moieties and to a water molecule. The last crystallographically different alkaline ion is K6B and this one is hexa-coordinated; this ion is linked to three POM units and two water molecules. All the corresponding distances are given as supplementary material in Table S4.

The above mentioned potassium ions do not present a preferential order along an axis or a particular plane. Figure 3 shows the coordination of the ions through water molecules, and also through the oxygen atoms of the vanadyl and borate fragments of the polyanionic ligand. This connectivity permits the generation of a 3D structure.

Structural description of $K_8Cs_2[V_{12}B_{18}O_{60}H_6]\cdot 10.40H_2O$ (4).

Dalton Transactions Accepted Manuscript

Crystalline lattice **4** contains two types of alkaline ions as charge compensating cations: potassium and caesium that are interacting with the BVO clusters, $[V_{12}B_{18}O_{60}H_6]^{10-}$. Six different crystallographic sites can be defined for the potassium ions and two for the caesium ions.

The first potassium ion is hepta-coordinated, bonded to two BVO clusters through four oxygen atoms from vanadyl groups, while the fifth and sixth coordination sites are occupied by bridging oxygen atoms (B_{trig}-O25-B_{tet}). The coordination sphere is completed by a water molecule. K2 is also hepta-coordinated; coordinating two oxygen atoms from vanadyl groups, one oxygen atom from a borate group (B_{trig}-O29), one bridging oxygen atom (B_{trig}-O21-B_{tet}) and three water molecules. K3 is hexa-coordinated, connecting two polyoxometalates; the coordination sphere is formed by six oxygen atoms from one vanadyl group, four bridges (B_{trig}-O30-B_{tet}; B_{tet}-O22-B_{tet}; V-O1-V; V-O6-V) and a water molecule. The hepta-coordination of K4 is similar to the one observed for K1. All the above mentioned potassium ions in **4** are connected to two clusters, while K5 is also connected to a third POM by only one bond, completing the coordination sphere by a water molecule. Finally, K6 is linked to only one BVO cluster. Table S5 summarizes all the above mentioned distances.

Figure S9 shows the *ac* plane and the coordination of K1 and K4 (some of the BVO species were omitted for clarity). K2, K3, K5 and K6 are out of the above mentioned plane.

The first caesium ion presents disorder, Cs1A/Cs1B, with partial occupancy of 0.42/0.08. The first coordination sphere of Cs1A is composed by eight oxygen atoms, one of which belongs to one BVO species, two correspond to a second BVO species, four to a third cluster and the eighth position is occupied by a water molecule (Figure 4a). The Cs2 ion is also octa-coordinated with

Dalton Transactions Accepted Manuscript

three oxygen atoms from one BVO cluster, and the rest of the coordination positions is completed by water molecules (Figure 4b; Table S6).

Comparative Description of the geometries around the alkaline ions.

The alkaline ions in frameworks **2** to **4** have different coordination numbers. The coordination sphere around the potassium ion can be described as hexa and hepta in **2**, **3,** and **4**. As expected, the caesium ion having a larger size presents the highest coordination number, being octa-coordinated in **4.** All these coordination numbers for the alkaline ions have been previously reported by Delgado et al.[58]. Using the SHAPE 2.1 program, developed by Alvarez et al.[46], it was possible to establish the best geometry for the existing potassium, and caesium ions**.** For compounds **2** and **3** the potassium ions adopt Octahedral (OC-6), Pentagonal Pyramid (PPY-6) and Capped Trigonal Prism (CTPR-7) geometries. For compound **4** the potassium ions adopt a Capped Trigonal Prism (CTPR-7), Capped Octahedral (COC-7) and Pentagonal Pyramid (PPY-6) geometries, whereas the caesium ions are hexagonal bipyramids (HBPY-8). The obtained geometries of the alkaline ions are shown in Figure 5.

Based on the Bond Valence Sum method (BVS) [59] and the crystallographic data, the mixed valence states of all the characterized clusters can be identified with the ratio of 10/2 (V^{IV}/V^{V}), since the calculated mean values were all close to the expected value of 4.17, for ten vanadium (IV) and two vanadium (V) centres [33]. The distortion degree of the vanadium atoms for all the clusters are similar, whether the vanadyl groups are interacting with the ammonium cations or with alkaline cations. A table with SHAPE[46] results is given in the supplementary material.

MAGNETIC PROPERTIES

Dalton Transactions Accepted Manuscript

Since all the studied lattices present clusters with the same mixed valence ratio, the magnetic response of only three of the frameworks (**1**, **2** and **3**) was measured. The magnetic properties of **1**, which corresponds to a framework with ammonium and 1,3-diapH_2 countercations, were compared to those of a framework with ammonium and potassium, **2**, and with that containing only potassium countercations, **3**.

The magnetic measurements for **1**, **2** and **3** were obtained in the temperature range of 2-300 K. Figures 6(a) and (b) show the $\chi_M T(T)$ curve, where it is possible to observe the lowering of the $\chi_M T$ product as the temperature decreases, permitting to infer a global antiferromagnetic behaviour for these frameworks.

Both **2** and **3** have similar $\chi_M T$ values at 300 and at 2 K (3.57 and 0.40 emu K mol^{-1} for **2,** and 3.58 and 0.38 emu K mol^{-1} for **3,** respectively). On the other hand, **1** presents a lower $\chi_M T$ value at room temperature and also at 2 K (3.34 and 0.33 emu K mol^{-1}). The calculated magnetic moment per vanadium centre for **2** and **3** is $\mu_{eff} = 1.69\mu_B$ at 300 K, being the value of $1.71\mu_B$ for vanadium (IV) with g =1.98. However, for **1** the calculated magnetic moment is $\mu_{eff} = 1.64\mu_B$ at 300 K, which is lower than the spin only value. All the $1/\chi_M(T)$ curves present a change of slope around 25 K. In all the curves a steeper decrease is observed in the range of 25 to 2 K. Using the temperature range of 25 to 300 K a value of the Weiss constant was estimated from the $1/\chi_M(T)$ curve, being θ = -112 for **1**, -73 K for **2** and -81 K for **3** (Figure 7). The abrupt change in the slope of the $1/\chi_M(T)$ curve may be rationalized due to different factors associated to these clusters: the presence of a great number of almost degenerate energy levels, being still populated under 25 K; the existence of a phase transition from a delocalized to a localized structure below

Dalton Transactions Accepted Manuscript

25 K (Class II Robin & Day classification) [60]; spin frustration due to the triangular arrangement of the spin carriers [61].

The system with alkaline ions as counter-cations presents an abated antiferromagnetism with respect to the systems with protonated amines as countercations (Figures 6(a) and (b)). This quenching effect was reported before by Müller et al.[35]. In this paper several new crystalline packing, derived from the fully reduced $[V_{18}O_{42}]$ polyanion with different countercations were described and magnetically studied. For example, the lattices $Cs_{11}[H_2V^{IV}_{18}O_{42}(SH)]\cdot 12H_2O$ and $Cs_{12}[V^{IV}_{18}O_{42}(H_2O)]\cdot 14H_2O$ contain the same number of spin carriers, however the reported $\chi_M T$ values per centre are 2.8 and 3.4 emu K mol^{-1} at 260 K respectively; therefore the effective magnetic moment per centre being 1.12 and 1.23 μ_B. An analysis of the crystalline lattices of both frameworks, shows that $Cs_{12}[V^{IV}_{18}O_{42}(H_2O)]\cdot 14H_2O$ presents a larger number of alkaline cation/vanadyl oxygen interactions than $Cs_{11}[H_2V^{IV}_{18}O_{42}(SH)]\cdot 12H_2O$ (being SH^- an occluded hydrogen sulphide anion). This fact permits to infer that the alkaline-vanadyl interactions quench the intracluster antiferromagnetic coupling.

Taking into account that the magnetic properties of the cluster are driven by the interaction between vanadyl groups bridged by oxido ligands, a more simple structure presenting both, magnetic coupling through oxido ligands and vanadyl groups, was chosen for DFT calculations of the magnetic interaction. In order to evaluate the effect of the alkaline ions on the magnetic properties of vanadyl containing systems, calculations were done on the dinuclear complex $[V_2O_2(\mu_2\text{-}OH)_2(1,4,7\text{-triazacyclononane})_2]^{2+}$ (CINKUF, CCDC code) [49]. Alkaline ions (Na^+ and K^+) at different distances of the oxygen atom of the vanadyl groups were considered in the calculations (See scheme).

Dalton Transactions Accepted Manuscript

The obtained results reflect that the calculated exchange interaction becomes less antiferromagnetic when the distance between M - $O_{vanadyl}$ ($M = Na^+, K^+$) becomes shorter (Figure 8a). The beta spin density of the oxygen atoms due to the polarization mechanism changes with the distance, and also the alpha spin density of the vanadium atoms. A lowering in the spin density values is observed when the distance between M - $O_{vanadyl}$ is decreased (Figures 8b and 8c), which is in agreement with the magnetic behaviour. It is clear that the effect of the positive charge of the alkaline ion is modifying the polarization mechanism in the metal atoms. This change on both, the alpha and beta spin densities, affects the magnitude of the exchange phenomena.

The overlap between the magnetic orbitals of both vanadium centres varies with the distance of the alkaline ion to the oxygen atom of the vanadyl group. It is clear that the presence of the alkaline ion produces a change on the extent of the magnetic orbitals, and therefore the overlap which determines the magnitude of the antiferromagnetic interaction (Figure 8d). Thus the DFT calculations have been able to give an explanation of the observed magnetic phenomena.

CONCLUSIONS

The characterized frameworks **1** to **4** are stabilized by hydrogen bond interactions, and/or by the coordinative interactions between the alkaline cations and the oxygen atoms of borate and vanadyl groups of the clusters. These interactions do not influence the number of absorption bands present in all the UV-visible spectra.

The cation – vanadyl interactions are shown to influence the magnitude of the intramolecular exchange interaction of the clusters, being the most coupled system the one that lacks alkaline

Dalton Transactions Accepted Manuscript

cations in the lattice, **1**. The observed quenching of the antiferromagnetic behaviour is strongest in the lattice which presents only alkaline cations in the intercluster space, **3**.

DFT calculations show that the positive charges strongly influence the polarization mechanism of the spin density of the vanadyl groups and the extent of the magnetic orbitals, therefore corroborating the experimental observation of the quenching effect of the magnetic coupling between vanadium centres.

ASSOCIATED CONTENT

Supporting Information

Additional figures, tables and X-ray crystallographic files in CIF format for compounds **1**, **2**, **3** and **4**.

AUTHOR INFORMATION

Corresponding Author

*E-mail: diego.venegas@usach.cl; Tel: (+)56-2-27181079

ACKNOWLEDGMENTS

Authors acknowledge FONDECYT 1120004 for financial support. This work was done under the LIA-MIF CNRS 836 Collaborative Program. PHI thanks MECESUP UCH 0601 Doctoral Scholarship. PHI also thanks CONICYT AT-24100222 and TT-23120099 Doctoral Scholarships. **Powered@NLHPC**: This research was partially supported by the supercomputing infrastructure of the NLHPC (ECM-02), Centre for Mathematical Modelling CMM, Universidad de Chile.

Dalton Transactions Accepted Manuscript

REFERENCES

1 I. A. Weinstock, *Chem. Rev.*, 1998, **98**, 113.

2 I. V. Kozhevnikov, *Chem. Rev.*, 1998, **98**, 171.

3 M. Sadakane and E. Steckhan, *Chem. Rev.*, 1998, **98**, 219.

4 A. Müller, F. Peters, M. T. Pope and D. Gatteschi, *Chem. Rev.*, 1998, **98**, 239.

5 E. Coronado and C. J. Gomez-García, *Chem. Rev.*, 1998, **98**, 273.

6 T. Yamase, *Chem. Rev.*, 1998, **98**, 307.

7 J. T. Rhule, C. L. Hill, D. A. Judd and R. F. Schinazi, *Chem. Rev.*, 1998, **98**, 327.

8 D. E. Katsoulis, *Chem. Rev.*, 1998, **98**, 359.

9 H. Zeng, G. R. Newkome and C. L. Hill, *Angew. Chem. Int. Ed*., 2000, **39**, 1771.

10 *Polyoxometalate Chemistry: from Topology via Self-assembly to Applications*, ed. M. T. Pope and A. Müller, Kluwer, Dordrecht, 2001.

11 A. M. Khenkin and R. Neumann, *J. Org. Chem*., 2002, **67**, 7075.

12 N. M. Okun, T. M. Anderson and C. L. Hill, *J. Am. Chem. Soc*., 2003, **125**, 3194.

13 M. V. Vasylyev and R. Neümann, *J. Am. Chem. Soc*., 2004, **126**, 884.

14 S. Liu, D. Volkmer and D. G. Kurth, *Anal. Chem*., 2004, **76**, 4579.

15 E. Coronado and P. Day, *Chem. Rev.*, 2004, **104**, 5419.

Dalton Transactions Accepted Manuscript

16 O. A. Kholdeeva, B. G. Donoeva, T. A. Trubitsina, G. Al-Kadamany and U. Kortz, *Eur. J. Inorg. Chem*., 2009, 5134.

17 B. G. Donoeva, T. A. Trubitsina, G. M. Maksimov, R. I. Maksimovskaya and O. A. Kholdeeva, *Eur. J. Inorg. Chem*., 2009, 5142.

18 C. Jahier, F.-X. Felpin, C. Méliet, F. Agbossou-Niedercorn, J.-C. Hierso and S. Nlate, *Eur. J. Inorg. Chem*., 2009, 5148.

19 J.-F. Lemonnier, S. Floquet, J. Marrot and E. Cadot, *Eur. J. Inorg. Chem*., 2009, 5233.

20 A. Dolbecq, E. Dumas, C. R. Mayer and P. Mialane, *Chem. Rev.*, 2010, **110**, 6009.

21 *Contemporary Boron Chemistry: Synthesis and Properties of Vanadoborate Cluster Materials*, ed., I. D. Williams, M. Wu, H. H.-Y. Song, T. S.-C. Law and X. X. Zhang, *The Royal Society of Chemistry*, 2000, 104.

22 I. D. Williams, M. Wu, H. H.-Y. Sung, X. X. Zhang and J. Yu, *Chem. Commun*., 1998, 2463.

23 Y.-N. Cao, H.-H. Zhang, C.-C. Huang, Y.-X. Sun, Y.-P. Chen, W.-J. Guo and F.-L. Zhang, *Chinese J. Struct. Chem*., 2005, **24**, 525.

24 Q. Cai, B. Lu, J. Zhang and Y. Shan, *J. Chem. Crystallogr*, 2008, **38**, 321.

25 Y. Cao, H. Zhang, C. Huang, Q. Yang, Y. Chen, R. Sun, F. Zhang and W. Guo, *J. Solid State Chem*., 2005, **178**, 3563.

26 C. J. Warren, R. C. Haushalter, D. J. Rose and J. Zubieta, *Inorg. Chim. Acta*, 1998, **282**, 123.

Dalton Transactions Accepted Manuscript

27 Y. Cao, H. Zhang, C. Huang, Y. Chen, R. Sun, and W. Guo, *J. Mol. Struct*., 2005, **733**, 211.

28 Y.-Q. Sun, G.-M. Li and Y.-P. Chen, *Dalton Trans*., 2012, **41**, 5774.

29 J. T. Rijssenbeek, D. J. Rose, R. C. Haushalter and J. Zubieta, *Angew. Chem. Int. Ed. Engl*., 1997, **36**, 1008.

30 Z.-H. Lin, Q.-Y. Yang, H.-H. Zhang, C.-C. Huang, R.-Q. Sun and X.-Y. Wu, *Chinese J. Struct. Chem*., 2004, **23**, 590.

31 B. Lu, H. Wang, L. Zhang, C.-Y. Dai, Q.-H. Cai and Y.-K. Shan, *Chin. J. Chem*., 2005, **23**, 137.

32 C. J. Warren, J. T. Rijssenbeek, D. J. Rose, R. C. Haushalter and J. Zubieta, *Polyhedron* 1998, **17**, 2599.

33 K. Brown, P. E. Car, A. Vega, D. Venegas-Yazigi, V. Paredes-García, M. G. F. Vaz, , R. A. Allao, J-Y. Pivan, E. Le Fur and E. Spodine, *Inorg. Chim. Acta*, 2011, **367**, 21.

34 C. J. Calzado, J. M. Clemente-Juan, E. Coronado, A. Gaita-Arino and N. Suaud, *Inorg. Chem*., 2008, **47**, 5889.

35 A. Müller, R. Sessoli, E. Krickemeyer, H. Bögge, J. Meyer, D. Gatteschi, L. Pardi, J. Westphal, K. Hovemeier, R. Rohlfing, J. Döring, F. Hellweg, C. Beugholt and M. Schmidtmann, *Inorg. Chem.,*1997, **36**, 5239.

36 J. Zhou, X. Liu, F. Hu, H. Zou and X. Li, *Inorg. Chem. Commun.*, 2012, **25**, 51.

37 SAINTPLUS Version 6.02, Brucker AXS: Madison, WI, 1999.

Dalton Transactions Accepted Manuscript

38 SHELXTL Version 5.1, Brucker AXS: Madison, WI, 1998.

39 G. M. Sheldrick, *ActaCryst*., 2008, **A64**, 112.

40 G. M. Sheldrick, SHELXL-97, *Program for Crystal Structure Refinement*, University of Göttingen, Germany, 1997.

41 G. R. Desiraju and T.Steiner, *The Weak Hydrogen Bond: In Structural Chemistry and Biology*, Oxford University, 2001.

42 K. Brandenburg, DIAMOND, Version 3.2i, Crystal Impact GbR, Bonn, Germany, 2012.

43 M. Pinsky and D. Avnir, *Inorg. Chem.,*1998, **37**, 5575.

44 D. Casanova, J. Cirera, M. Llunell, P. Alemany, D. Avnir, and S. Alvarez, *J. Am. Chem. Soc.,* 2004, **126**, 1755.

45 J. Cirera, E. Ruiz and S. Alvarez, *Chem., Eur. J.* 2006, **12**, 3162.

46 M. Llunell, D. Casanova, J. Cirera, P. Alemany and S. Alvarez, D. *SHAPE*, version 2.1, Barcelona, Spain, 2013.

47 W. W. Wendlandt and H. G. Hecht, Reflectance Spectroscopy, Wiley-Interscience, New York, 1966.

48 G. A. Bain and J. F. Berry, *J. Chem. Educ.*, 2008, **85**, 532.

49 K. Wieghardt, U. Bossek, K. Volckmar, W. Swiridoff and J. Weiss, *Inorg. Chem.*, 1984, **23**, 1387.

50 A. D. Becke, *J. Chem. Phys.,*1993, **98**, 5648.

Dalton Transactions Accepted Manuscript

51 A. Schafer, C. Huber and R. Ahlrichs, *J. Chem. Phys.*, 1994, **100**, 5829.

52 Jaguar, version 5.5 Schrödinger, LLC: Portland, OR, USA, 2003.

53 M. J. Frisch, G. W. Trucks, H. B. Schlegel, G. E. Scuseria, M. A. Robb, J. R. Cheeseman, J. A. Montgomery, T. Vreven, K. N. Kudin, J. C. Burant, J. M. Millam, S. S. Iyengar, J. Tomasi, V. Barone, B. Mennucci, M. Cossi, G. Scalmani, N. Rega, G. A. Petersson, H. Nakatsuji, M. Hada, M. Ehara, K. Toyota, R. Fukuda, J. Hasegawa, H. Ishida, T. Nakajima, Y. Honda, O. Kitao, H. Nakai, M. Klene, X. Li, J. E. Knox, H. P. Hratchian, J. B. Cross, C. Adamo, J. Jaramillo, R. Gomperts, R. E. Stratmann, O. Yazyev, A. J. Austin, R. Cammi, C. Pomelli, J. Ochterski, P. Y. Ayala, K. Morokuma, G. A. Voth, P. Salvador, J. J. Dannenberg, V. G. Zakrzewski, S. Dapprich, A. D. Daniels, M. C. Strain, O. Farkas, D. K. Malick, A. D. Rabuck, K. Raghavachari, J. B. Foresman, J. V. Ortiz, Q. Cui, A. G. Baboul, S. Clifford, J. Cioslowski, B. B. Stefanov, G. Liu, A. Liashenko, P. Piskorz, I. Komaromi, R. L. Martin, D. J. Fox, T. Keith, M. A. Al-Laham, C. Y. Peng, A. Nanayakkara, M. Challacombe, P. M. W. Gill, B. Johnson, W. Chen, M. W. Wong, C. Gonzalez and J. A. Pople, In Gaussian 09 (Revision D.2), Gaussian, Inc., Pittsburgh, PA, USA, 2009.

54 E. Ruiz, *Struct. Bond.,* 2004, **113**, 71.

55 P. Hermosilla-Ibáñez, P. E. Car, A. Vega, J. Costamagna, F. Caruso, J.-Y. Pivan, E. Le Fur, E. Spodine and D. Venegas-Yazigi, *CrystEngComm*., 2012, **14**, 5604.

56 J. Zhou, X. Liu, F. Hu, H. Zou, R. Li and X. Li, *RSC Advances*, 2012, **2**, 10937.

57 X. Liu, J. Zhou, Z. Zhou and F. Zhang, *J. Clust. Sci*., 2011, **22**, 65.

Dalton Transactions Accepted Manuscript

58 F. S. Delgado, C. Ruiz-Pérez, J. Sanchiz, F. Lloret and M. Julve, *CrystEngComm.*, 2006, **8**, 507.

59 I. D. Brown and D. Altermatt. *Acta Cryst.,*1985, **B41**, 244.

60 M. B. Robin and P. Day, *Adv. Inorg. Chem. RadioChem.*, 1967, **10**, 247.

61 P. Kögerler, B. Tsukerblat and A. Müller, *Dalton Trans.*, 2010, **39**, 21.

Dalton Transactions Accepted Manuscript

Figure 1. UV-vis reflectance spectra for **1**, **2**, **3**, and **4**.

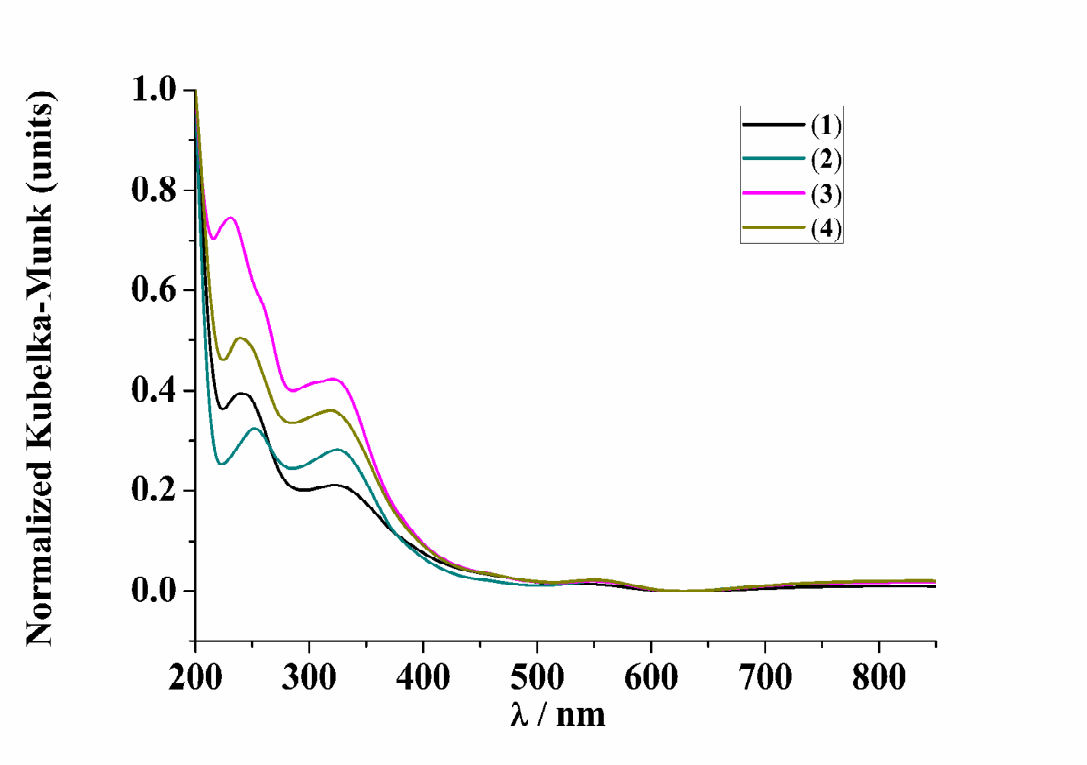

Dalton Transactions Accepted Manuscript

Figure 2. View of the crystalline packing of **1** in the plane (0 $\bar{1}$ 0).

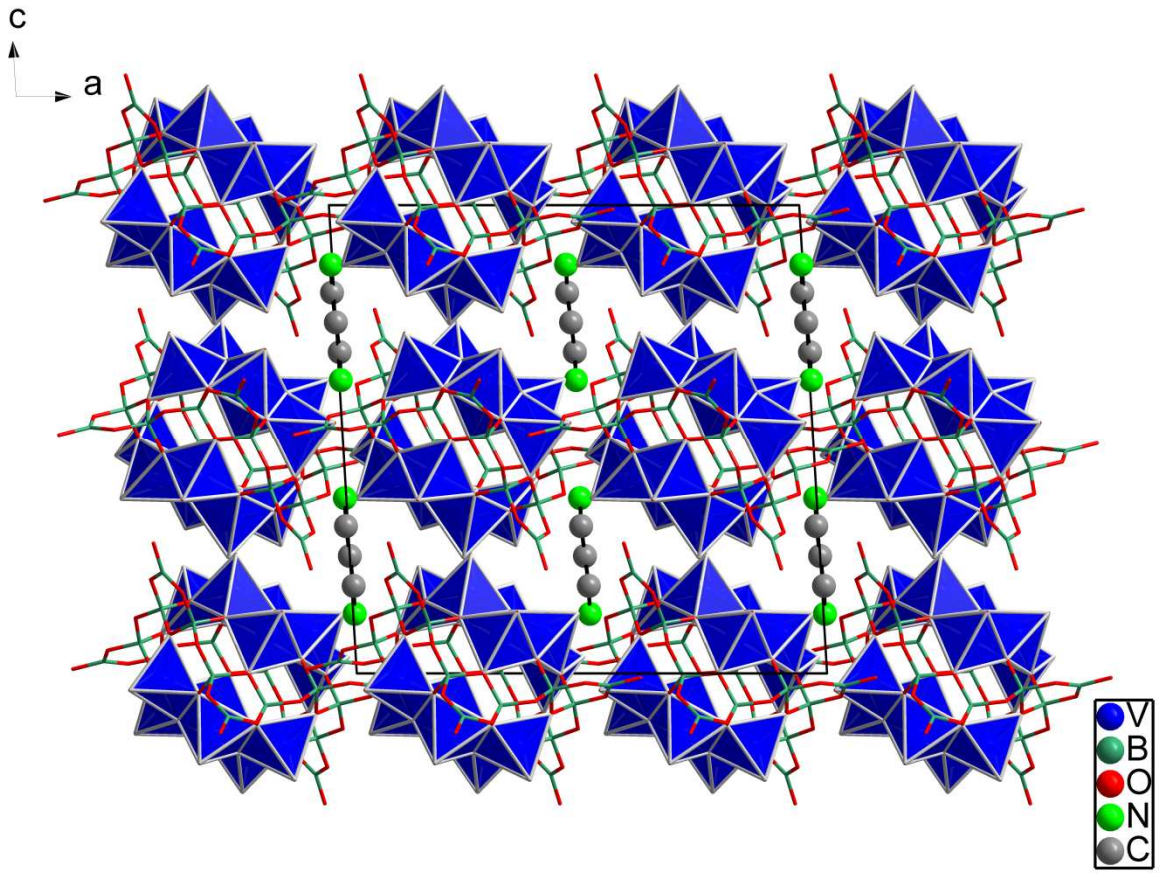

Dalton Transactions Accepted Manuscript

Figure 3. Coordination sphere of K1, K2A, K3, K4, K5 and K6B for **3**.

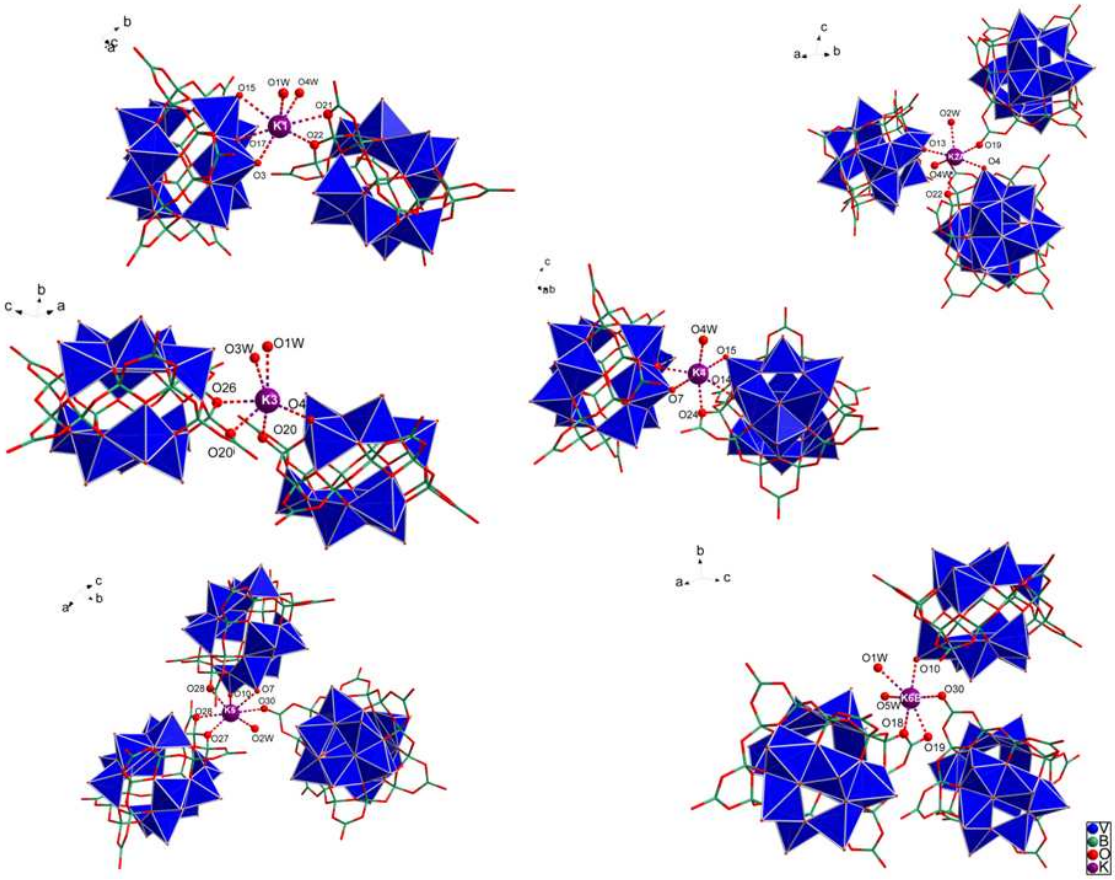

Dalton Transactions Accepted Manuscript

Figure 4. Coordination sphere of Cs1A and Cs2 for **4**.

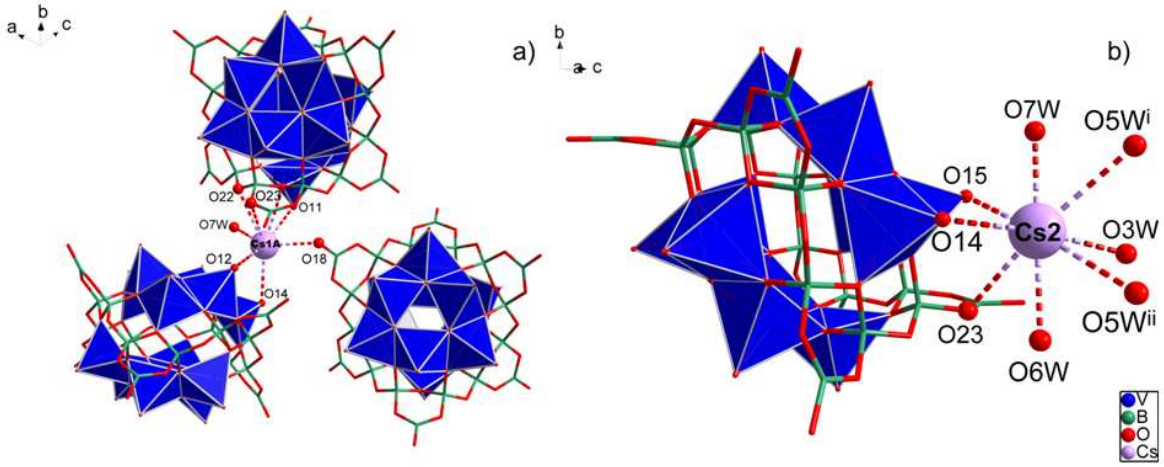

Dalton Transactions Accepted Manuscript

Figure 5. The different geometries of the K and Cs ions for compounds **2**, **3** and **4**; OC-6 (Octahedron), PPY-6 (Pentagonal Pyramid), PBPY-7 (Pentagonal Bipyramid), COC-7 (Capped Octahedron), CTPR-7 (Capped Trigonal Prism) and HBPY-8 (Hexagonal Bipyramid).

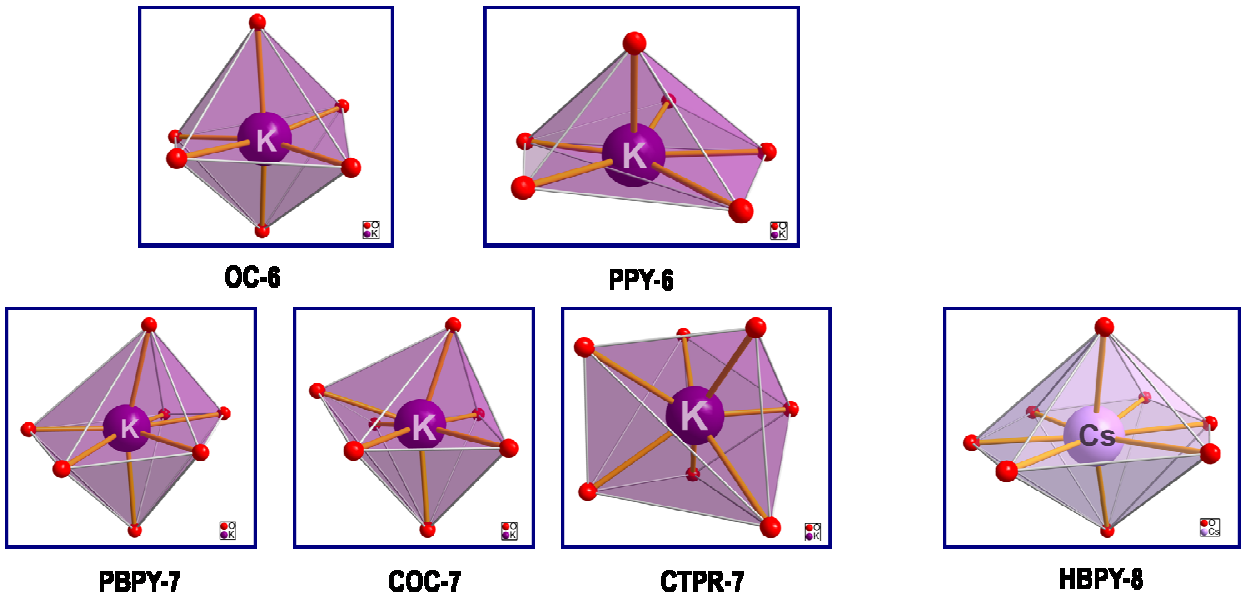

Dalton Transactions Accepted Manuscript

Figure 6. Thermal dependence of χT for (a) **1** (green triangles) and **2** (red circles); for (b) **1** (green triangles) and **3** (blue squares).

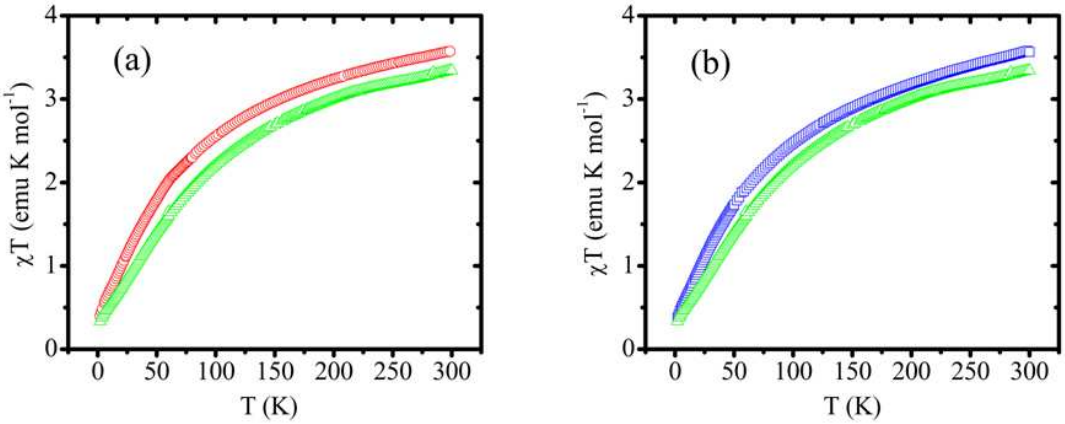

Dalton Transactions Accepted Manuscript

Figure 7. Thermal dependence of 1/χ for **1** green triangles; for **2** red circles; for **3** blue squares.

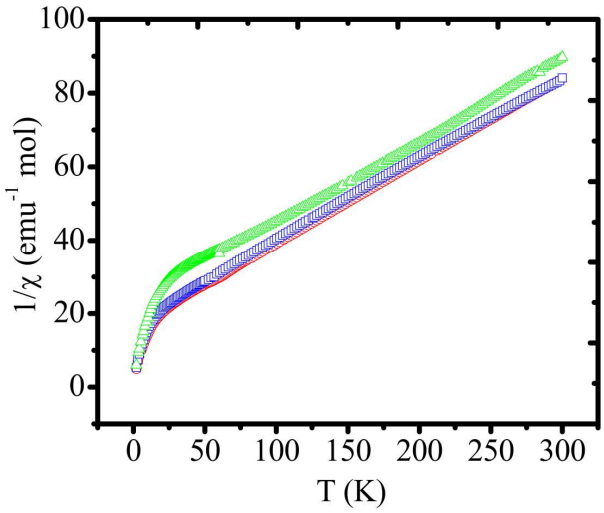

Dalton Transactions Accepted Manuscript

Figure 8. (a) Dependence of the magnitude of the exchange interaction with the distance of M^+ to the oxygen atoms of the vanadyl groups (circles Na; triangles K); (b) and (c) Dependence of the spin density values of the vanadium(IV) and the oxygen atoms of the vanadyl groups with the different distances of Na^+ to the oxygen atoms of the vanadyl groups; (d) dependence of the magnitude of the overlap of the magnetic orbitals with the different distances.

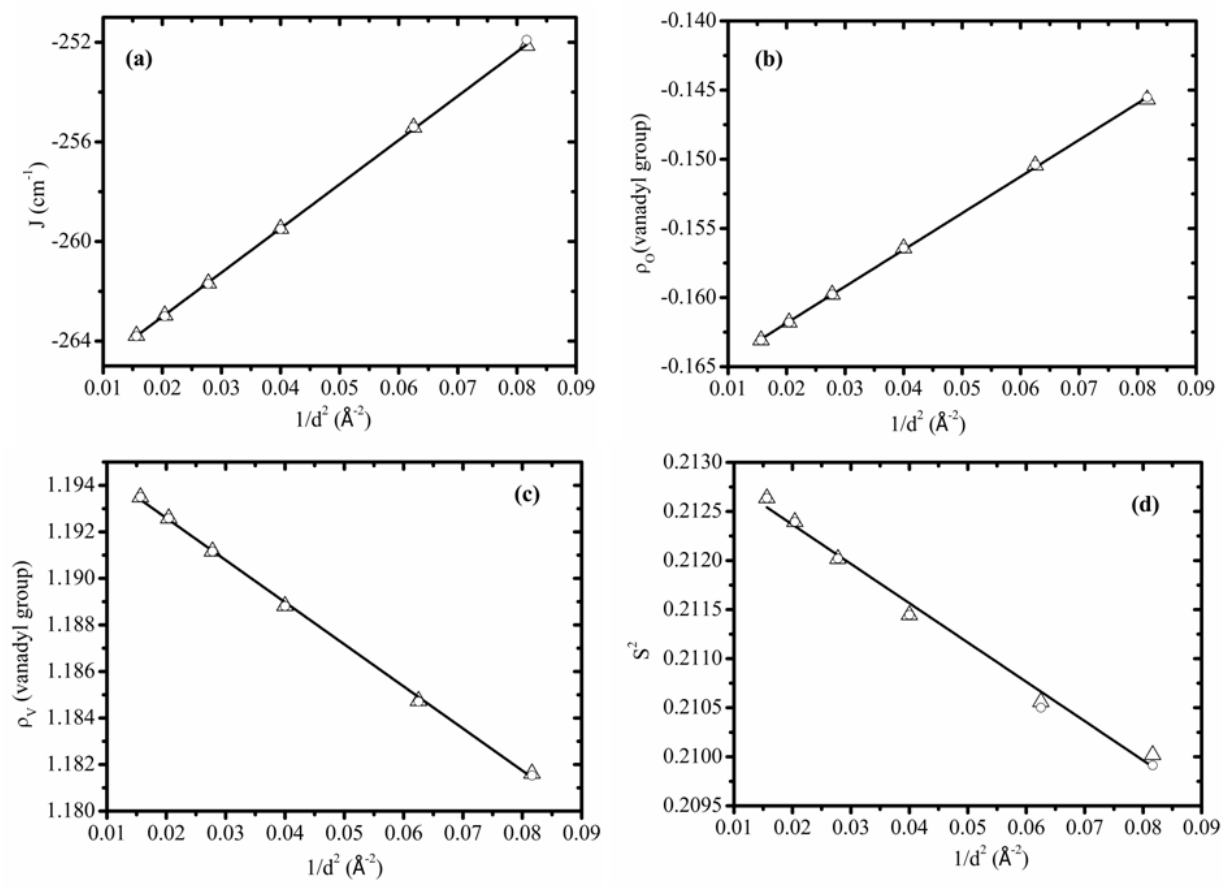

Dalton Transactions Accepted Manuscript

Scheme. Position of the alkaline ions with respect to the oxygen atoms of the vanadyl groups, used in DFT calculations.

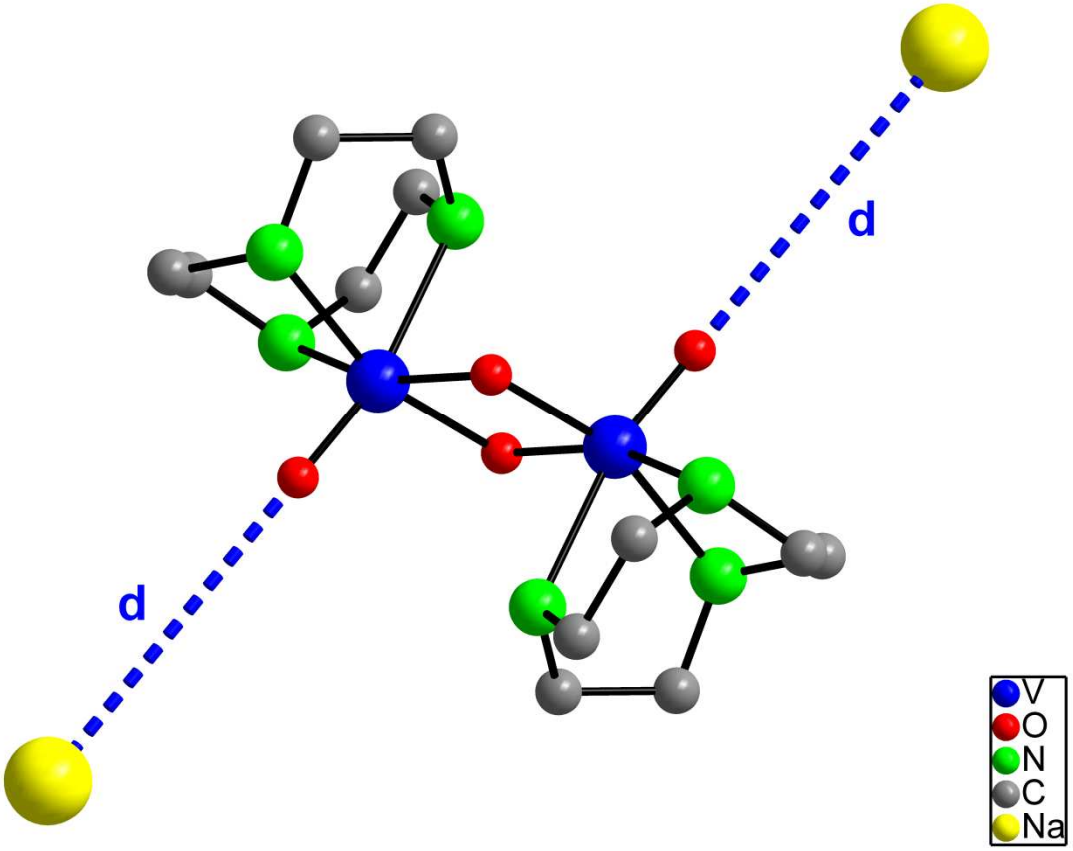

Dalton Transactions Accepted Manuscript

Table 1. Crystal data and structure refinement for complexes 1-4.

Complex	**1**	**2**	**3**	**4**
Formula	$C_3H_{60.48}B_{18}N_{10}O_{65.24}V_{12}$	$B_{18}H_{50}K_8N_2O_{78}V_{12}$	$B_{18}H_{25}K_{10}O_{69.50}V_{12}$	$B_{18}Cs_2H_{26.8}K_8O_{70.40}V_{12}$
Moiety formula	$(NH_4)_8$(1,3-diapH_2)$[V_{12}B_{18}O_{60}H_6]\cdot 5.24H_2O$	$K_8(NH_4)_2[V_{12}B_{18}O_{60}H_6]\cdot 18.00H_2O$	$K_{10}[V_{12}B_{18}O_{60}H_6]\cdot 9.50H_2O$	$K_8Cs_2[V_{12}B_{18}O_{60}H_6]\cdot 10.40H_2O$
Formula weight	2086.84	2445.08	2334.06	2537.90
Temperature (K)	293(2)	293(2)	293(2)	297(2)
Crystal system	Monoclinic	Orthorhombic	Monoclinic	Monoclinic
Space group	$C2/_C$	*Pbca*	$P2_1/n$	*C2/c*
a (Å)	19.5778(19)	19.1919(18)	13.1294(19)	19.4188(14)
b (Å)	18.3702(17)	18.1864(17)	19.973(3)	18.6745(14)
c (Å)	19.5431(19)	19.2584(18)	13.4315(19)	19.3128(14)
α (º)	90.00	90.00	90.00	90.00
β (º)	93.406(2)	90.00	115.079(2)	91.9440(10)
γ (º)	90.00	90.00	90.00	90.00
Volume ($Å^3$)	7016.2(12)	6721.8(11)	3190.1(8)	6999.5(9)
Z	4	8	4	2
Density (calculated) ($g\cdot cm^{-3}$)	1.935	2.366	2.404	2.383
Absorption coefficient (mm^{-1})	1.647	2.231	2.462	3.153
F(000)	3975.7	4624.0	2224.0	4764.8
Crystal size (mm^3)	0.25 × 0.19 × 0.15	0.30 × 0.26 × 0.23	0.14 × 0.12 × 0.11	0.37 × 0.20 × 0.13
θ range for data collection (º)	1.52 to 26	1.87 to 26	1.82 to 26	1.51 to 24.99
Index ranges	$-24\le h\le 24$, $-22\le k\le 22$, $-24\le l\le 24$	$-23 \le h \le 23$ $-22 \le k \le 22$ $-23 \le l \le 23$	$-15 \le h \le 16$ $-24 \le k \le 24$ $-16 \le l \le 16$	$-22 \le h \le 23$ $-22 \le k \le 22$ $-22 \le l \le 11$
Reflections collected	23524	43698	24885	14181
Independent reflections	6904[R(int) = 0.0445]	6616[R(int) = 0.0367]	6275[R(int) = 0.0389]	6148[R(int) = 0.0257]
Refinement method	Full-matrix least-squares on F2	Full-matrix least-squares on F2	Full-matrix least-squares on F2	Full-matrix least-squares on F2
Goodness-of-fit on F^2	1.073	1.135	1.108	1.066
Final R indices [I>2sigma(I)]	$R_1 = 0.0638$, $wR_2 = 0.2038$	$R_1 = 0.0644$, $wR_2 = 0.1835$	$R_1 = 0.0547$, $wR_2 = 0.1650$	$R_1 = 0.0770$, $wR_2 = 0.2264$
R indices (all data)	$R_1 = 0.0743$, $wR_2 = 0.2119$	$R_1 = 0.0701$, $wR_2 = 0.1900$	$R_1 = 0.0659$, $wR_2 = 0.1759$	$R_1 = 0.0837$, $wR_2 = 0.2358$
Largest diff. peak and hole e.$Å^{-3}$	2.96 and -0.51	2.38/-1.20	1.83/-0.88	3.52/-1.11

Dalton Transactions Accepted Manuscript

Graphical Abstract

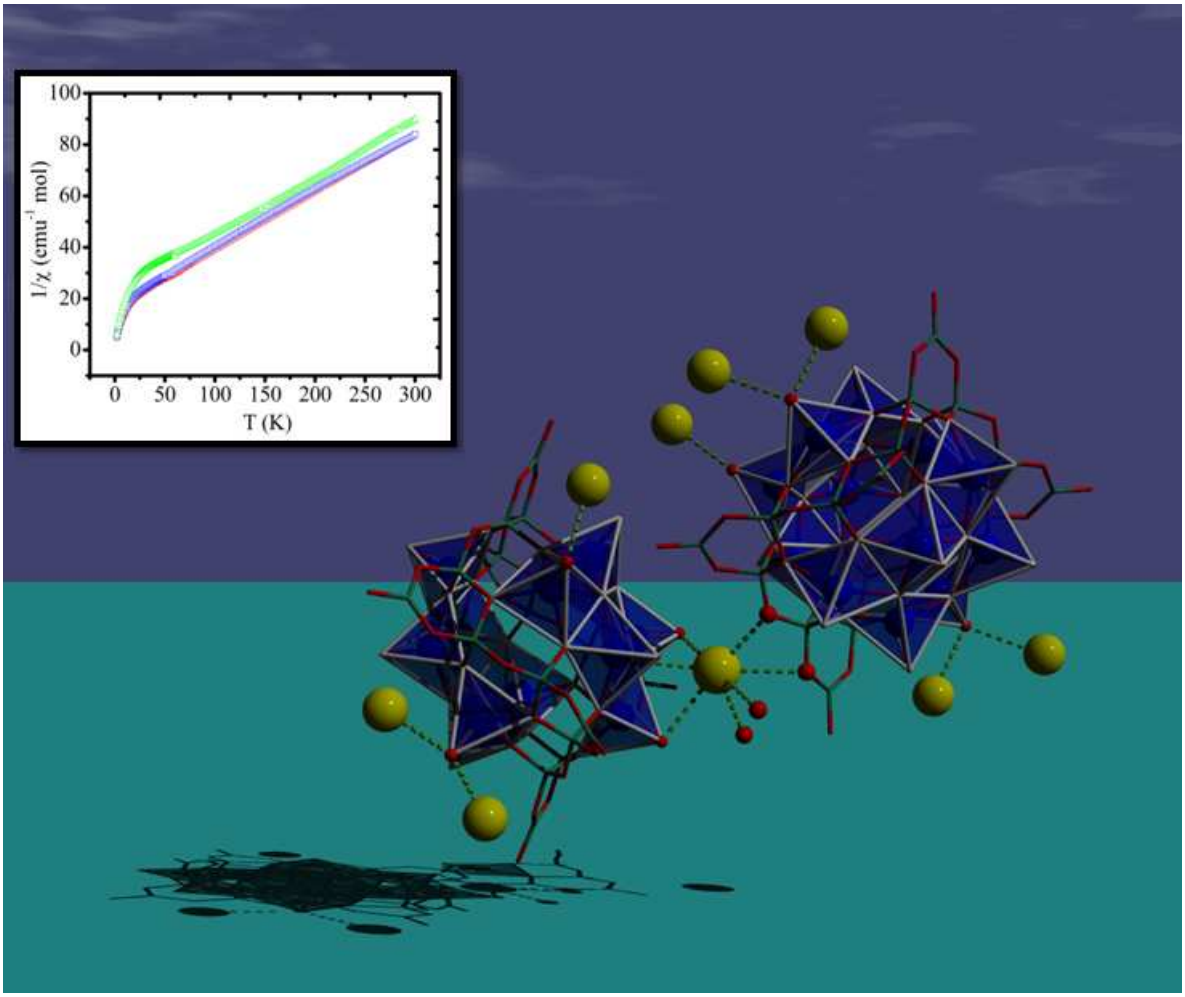

Quenching effect of the intracluster antiferromagnetic coupling by alkaline ions of the crystalline packing.

Dalton Transactions Accepted Manuscript